

Article

Warm White Light-Emitting Diodes Based on a Novel Orange Cationic Iridium(III) Complex

Huaijun Tang *, Guoyun Meng, Zeyu Chen, Kaimin Wang, Qiang Zhou and Zhengliang Wang *

Key Laboratory of Comprehensive Utilization of Mineral Resources in Ethnic Regions, Joint Research Centre for International Cross-border Ethnic Regions Biomass Clean Utilization in Yunnan, School of Chemistry & Environment, Yunnan Minzu University, Kunming 650500, China; mengguoyun@sina.com (G.M.); chenzy1120@163.com (Z.C.); kmwang041684@163.com (K.W.); xchow123@126.com (Q.Z.)

* Correspondence: tanghuaijun@sohu.com (H.T.); wzhl629@163.com (Z.W.); Tel./Fax: +86-871-6591-0017 (H.T.)

Received: 19 April 2017; Accepted: 8 June 2017; Published: 16 June 2017

Abstract: A novel orange cationic iridium(III) complex [(TPTA)₂Ir(dPPOA)]PF₆ (TPTA: 3,4,5-triphenyl-4*H*-1,2,4-triazole, dPPOA: N,N-diphenyl-4-(5-(pyridin-2-yl)-1,3,4-oxadiazol-2-yl)aniline) was synthesized and used as a phosphor in light-emitting diodes (LEDs). [(TPTA)₂Ir(dPPOA)]PF₆ has high thermal stability with a decomposition temperature (*T_d*) of 375 °C, and its relative emission intensity at 100 °C is 88.8% of that at 25 °C. When only [(TPTA)₂Ir(dPPOA)]PF₆ was used as a phosphor at 6.0 wt % in silicone and excited by a blue GaN (GaN: gallium nitride) chip (450 nm), an orange LED was obtained. A white LED fabricated by a blue GaN chip (450 nm) and only yellow phosphor Y₃Al₅O₁₂:Ce³⁺ (YAG:Ce) (1.0 wt % in silicone) emitted cold white light, its CIE (CIE: *Commission Internationale de l'Eclairage*) value was (0.32, 0.33), color rendering index (CRI) was 72.2, correlated color temperature (CCT) was 6877 K, and luminous efficiency (*η_L*) was 128.5 lm·W^{−1}. Such a cold white LED became a neutral white LED when [(TPTA)₂Ir(dPPOA)]PF₆ was added at 0.5 wt %; its corresponding CIE value was (0.35, 0.33), CRI was 78.4, CCT was 4896 K, and *η_L* was 85.2 lm·W^{−1}. It further became a warm white LED when [(TPTA)₂Ir(dPPOA)]PF₆ was added at 1.0 wt %; its corresponding CIE value was (0.39, 0.36), CRI was 80.2, CCT was 3473 K, and *η_L* was 46.1 lm·W^{−1}. The results show that [(TPTA)₂Ir(dPPOA)]PF₆ is a promising phosphor candidate for fabricating warm white LEDs.

Keywords: cationic iridium(III) complex; warm whitelight-emitting diode; photoluminescence; blue GaN chip; YAG:Ce

1. Introduction

Due to high efficiency, long lifetime, and energy-saving and environmentally-friendly properties, white light-emitting diodes (WLEDs) have attracted significant attention and are used as the new generation solid-state light sources in general illumination, full-color displays, liquid crystal display backlights and so on [1–4]. At present, the commercial WLEDs are mainly obtained by the combination of a blue GaN (GaN: gallium nitride) chip (*λ_{max,em}* ≈ 450 nm) and a yellow-emitting Y₃Al₅O₁₂:Ce³⁺ (YAG:Ce) phosphor. YAG:Ce is a blue-light excitable phosphor with high photoluminescence efficiency and good thermal stability [4–6]. However, because the main emission of YAG:Ce is in the greenish yellow region, aforementioned commercial WLEDs have low color rendering index (CRI) and high correlated color temperature (CCT). Due to the absence of a red light component in their spectra, the light emitted from such WLEDs is cold white light [7–16]. Two approaches have been developed to overcome this drawback. In the first approach, a red light component was emitted via some ions (such as Eu³⁺, Pr³⁺) being doped in YAG:Ce [7–9]; however, the yellow emission was obviously decreased although slightly red light was obtained. In the other approach, some red phosphors were complementally used in aforementioned WLEDs [5,9,10]. Relatively better performances (including

CRI, CCT and efficiency etc.) can be obtained via the second approach, because the red phosphors are mainly excited by the blue GaN chip and the emission of YAG:Ce is seldom affected. Hence, the development of new efficient red phosphors for warm WLEDs based on blue chips is very important and urgently needed. Up to now, besides many inorganic phosphors (such as $\text{CaSiAlN}_3\text{:Eu}^{2+}$ [10], InP/GaP/ZnS quantum dots [11], Mn^{4+} activated fluorides [5,12,13], and so on), many organic luminescent materials (such as organic metal complexes [14–18], polymers [19] and small-molecule fluorescent dyes [20,21], and so on) have also been used as red luminescent materials in WLEDs.

Up to now, many types of organic metal complexes (e.g., cationic ruthenium(II) complexes, cationic copper(I) complexes, europium(III) complexes, platinum(II) complexes, zinc(II) complexes, etc.) have been used in various luminescent fields. By comparison, as efficient luminescent materials, cationic iridium(III) complexes have some excellent photochemical and photophysical properties, such as high efficiency of 100% theoretical quantum efficiency, good color tenability via various ligands, short triplet state lifetimes, high thermal and photic stability and so on [22,23]. In the past decade and even earlier, cationic iridium(III) complexes have been widely applied in light-emitting electrochemical cells (LECs) [22–24], organic light-emitting diodes (OLEDs) [24–26], chemical sensors [27], and bioimaging [28] etc.

Recently, cationic iridium(III) complexes have also been used as luminescence conversion materials (i.e., phosphors) in inorganic LEDs [15,18,29,30], and exhibited good performances. In 2013, C.-Y. Sun et al. [29] achieved efficient white-light emission by encapsulating the cation of a yellow-emitting iridium complex $[\text{Ir}(\text{ppy})_2(\text{bpy})]\text{PF}_6$ (ppy: 2-phenylpyridine; bpy: 2,2'-bipyridine) at different ratios in the blue-emitting anionic Cd-based metal–organic frameworks (MOF) cavity. When an optimal concentration (3.5 wt %) of $[\text{Ir}(\text{ppy})_2(\text{bpy})]^+$ was encapsulated into the host framework and under the excitation of 370 nm ultraviolet light, high-quality white light was obtained with Commission International de l'Éclairage (CIE) coordinates of (0.31, 0.33), a CRI of ca. 80, a CCT of ca. 5900 K, and a quite high quantum yield up to 20.4%. Then high-quality WLEDs were fabricated by using this composite material and ultraviolet chips. In 2016, L. Niklaus et al. [18] fabricated white hybrid light-emitting diodes (WHLEDs) using luminescent rubber-like materials based on a wide palette of compounds including small-molecules, quantum dots, polymers, and coordination complexes. The use of rubbers based on the complex $[\text{Ir}(\text{ppy})_2(\text{tb-bpy})]\text{PF}_6$ (tb-bpy: 4,4'-ditert-butyl-2,2'-bipyridine) outperformed the others in terms of color quality (CRI > 80) and luminous efficiency ($>100 \text{ lm}\cdot\text{W}^{-1}$) with unprecedented stabilities of more than 1000 h (extrapolated 4000 h) under continuous operation conditions. In one reported work of our research group in 2015 [30], WLEDs fabricated by using cationic iridium(III) complexes $[\text{Ir}(\text{ppy})_2(\text{phen})]\text{PF}_6$ or $[\text{Ir}(\text{ppy})_2(\text{phen})]\text{TiF}_6$ (phen: 1,10-phenanthroline) as luminescence conversion materials showed higher CRI and lower CCT than those of the widely used YAG:Ce. In another reported work of our research group also in 2015 [15], a novel red-emitting cationic iridium(III) complex using 2-(9-(2-ethylhexyl)-9H-carbazol-3-yl)benzo[d]thiazole (CBT) as the main ligand and N,N-diphenyl-4-(5-(pyridin-2-yl)-1,3,4-oxadiazol-2-yl)aniline (dPPOA) as the auxiliary ligand was used as a red phosphor in YAG:Ce based WLEDs with 465 nm-emitting GaN blue chips. The WLED only using YAG:Ce as a phosphor at 1.0 wt % emitted cold white; such WLED can become warm WLEDs when the cationic iridium(III) complex was added over 1.0 wt %.

As a consecutive and upgraded research by us, in this work, another novel orange cationic iridium(III) complex also using dPPOA as auxiliary ligand, but using 3,4,5-triphenyl-4H-1,2,4-triazole (TPTA) instead of CBT as the main ligand was synthesized and also used in YAG:Ce-based WLEDs to obtain warm white light. Donor–acceptor bipolar units have been widely used in organic photoresponse materials for extending absorption range and increasing absorption rate [25,31,32]. Many organic cationic iridium(III) complexes can easily be excited by ultraviolet light, but cannot be effectively excited by blue light (such as the blue light of a GaN chip). In order to make this new complex effectively excited by the blue light of a GaN chip, a donor–acceptor bipolar unit of triphenylamine–oxadiazole was contained in the auxiliary ligand dPPOA; theoretically, the electron-donating or/and electron-withdrawing functional groups on the main ligand will further

improve the effect of this donor–acceptor bipolar unit [31,32]. In our previous work [15], CBT containing an electron-donating carbazole group had been successfully used in the cationic iridium(III) complex $[\text{Ir}(\text{CBT})_2(\text{dPPOA})]\text{PF}_6$ for warm WLEDs. This work tried the main ligand TPTA containing an electron-withdrawing 1,2,4-triazole group. In order to achieve higher performance in this new work, besides the replacement of the main ligand in the complex as a new attempt, 450 nm-emitting GaN blue chips with much higher luminous efficiency were also used to replace the 465 nm-emitting GaN blue chips used in previous work [15]. As expected, the cold white light of YAG:Ce-based WLEDs also gradually became warm white light with the increase of the addition of this new cationic iridium(III) complex; at the same time, such WLEDs exhibited encouraging light-emitting performances.

2. Materials and Methods

2.1. General Information

All chemicals and reagents were purchased from chemical reagent companies and used without further purification unless otherwise stated. ^1H NMR spectra were recorded on a Bruker AV400 spectrometer (Bruker, Fällanden, Switzerland) operating at 400 MHz; tetramethylsilane (TMS) was used as internal standard. Mass spectra (MS) were obtained on a Bruker amaZon SL liquid chromatography mass spectrometer (LC-MS, Bruker, Karlsruhe, Germany) with an electrospray ionization (ESI) interface using acetonitrile as matrix solvent. Elemental analysis (EA) was performed on a Vario EL III Elemental Analysis Instrument (Elementar, Hanau, Germany). Ultraviolet-visible (UV-vis, Agilent, Palo Alto, CA, USA) absorption spectra were measured on an Agilent 8453 UV-visible Spectroscopy System. Excitation and emission spectra of samples were documented on a Cary Eclipse FL1011M003 (Varian, Palo Alto, CA, USA) spectrofluorometer; the xenon lamp was used as an excitation source, and the temperature of solid samples was controlled by a temperature controller (REX-C110, Kaituo Compressor Parts Co., Ltd, Dongguan, China). Thermogravimetric (TG) analysis was carried out up to 600 °C in N_2 atmosphere with a heating speed of $10.0\text{ }^\circ\text{C}\cdot\text{min}^{-1}$ on a NETZSCH STA 449F3 thermogravimetric analyzer (NETZSCH, Selb, Germany). The electroluminescent spectra of LEDs were recorded on a high-accuracy array spectrometer (HSP6000, HongPu Optoelectronics Technology Co., Ltd, Hangzhou, China).

2.2. Synthesis

The cationic iridium(III) complex $[(\text{TPTA})_2\text{Ir}(\text{dPPOA})]\text{PF}_6$ was synthesized by using 3,4,5-triphenyl-4H-1,2,4-triazole (TPTA) and N,N-diphenyl-4-(5-(pyridin-2-yl)-1,3,4-oxadiazol-2-yl)aniline (dPPOA) as ligands, as shown in Figure 1. TPTA and dPPOA were synthesized according to the reported procedures in references [33] and [15] respectively.

Synthesis of the chloro-bridged dimer $(\text{TPTA})_2\text{Ir}(\mu\text{-Cl})_2\text{Ir}(\text{TPTA})_2$: A mixture of $\text{IrCl}_3\cdot 3\text{H}_2\text{O}$ (1.06 g, 3.0 mmol) and TPTA (1.81 g, 6.10 mmol) in H_2O (10 mL) and 2-methoxyethanol (30 mL) was refluxed in Ar atmosphere for 24 h. After being cooled to room temperature, the resultant yellow precipitate was collected on a filter, washed with water and methanol alternately, and then dried in a vacuum. Yield was 75.0% (1.85 g) yellow solid. This dimer product was directly used for the next step without further purification and characterization.

Synthesis of the cationic iridium(III) complex $[(\text{TPTA})_2\text{Ir}(\text{dPPOA})]\text{PF}_6$: The chloro-bridged dimer $(\text{TPTA})_2\text{Ir}(\mu\text{-Cl})_2\text{Ir}(\text{TPTA})_2$ (0.62 g, 0.38 mmol) and dPPOA (0.30 g, 0.76 mmol) were added into glycol (30 mL) and then kept at 150 °C in Ar atmosphere with stirring for 16 h. After being cooled to room temperature, 10 mL $1.0\text{ mol}\cdot\text{L}^{-1}$ aqueous solution of NH_4PF_6 was added with stirring, and much orange flocculent precipitate appeared. The precipitate was filtered, washed with water and dried in a vacuum. The crude product was purified by column chromatography on silica gel, eluting with $\text{CH}_2\text{Cl}_2/\text{MeCN}$ (volume rate, 10:1). Yield was 86.0% (0.86 g) orange solid. ^1H NMR (400 MHz, CDCl_3 , 25 °C, ppm, being shown in Figure S1 as electronic supplementary materials), δ : 8.50 (d, 1H, $^3J = 7.6\text{ Hz}$, ArH), δ : 8.33–8.63 (m, 1H, ArH), δ : 8.16 (d, 1H, $^3J = 5.6\text{ Hz}$, ArH), δ : 7.97–7.99 (m, 2H, ArH), δ : 7.62–7.69

(m, 7H, ArH), δ : 7.47–7.53 (m, 4H, ArH), δ : 7.31–7.39 (m, 11H, ArH), δ : 7.23–7.27 (m, 3H, ArH), δ : 7.14–7.18 (m, 6H, ArH), δ : 7.04–7.06 (m, 2H, ArH), δ : 6.91–7.00 (m, 2H, ArH), δ : 6.75–6.78 (m, 2H, ArH), δ : 6.71 (t, 1H, $^3J = 7.6$ Hz, ArH), δ : 6.66 (d, 1H, $^3J = 7.2$ Hz, ArH), δ : 6.44 (t, 2H, $^3J = 7.6$ Hz, ArH). MS (m/z , ESI⁺, being shown in Figure S2 as electronic supplementary materials): calc. for C₆₅H₄₆F₆IrN₁₀OP, 1320.3, found, 1175.3 [M–PF₆]⁺. Element analysis calculation for C₆₅H₄₆F₆IrN₁₀OP: C, 59.13; H, 3.51; N, 10.61%. Found: C, 58.69; H, 3.67; N, 9.91%.

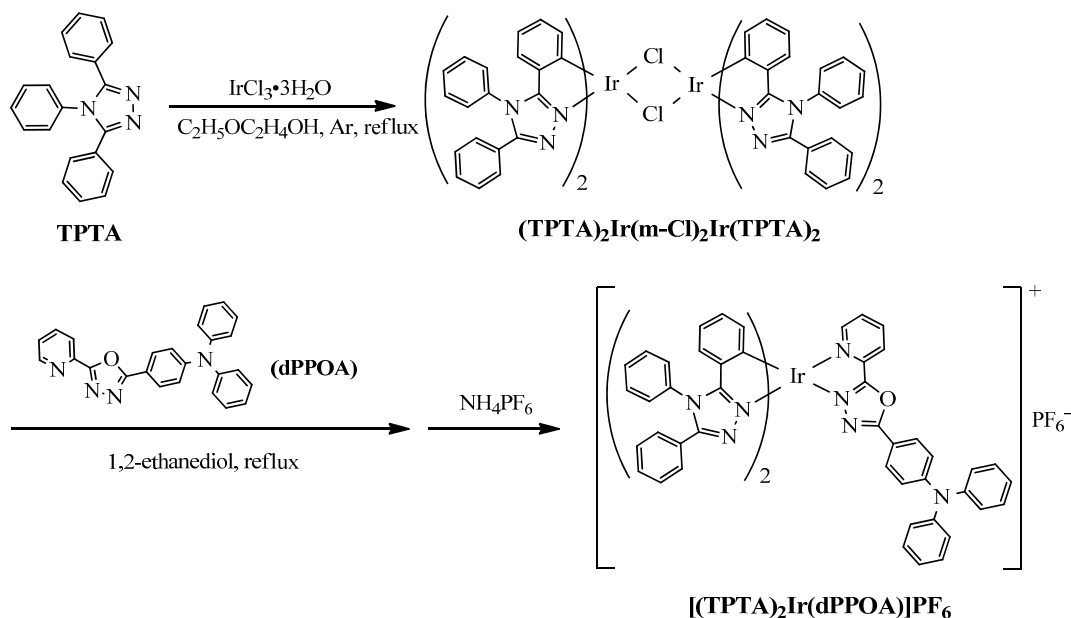


Figure 1. Synthetic route and chemical structure of [(TPTA)₂Ir(dPPOA)]PF₆.

2.3. Fabrication and Measurements of LEDs

Two kinds of LEDs were fabricated and measured in this work. (i) Only [(TPTA)₂Ir(dPPOA)]PF₆ was blended and stirred homogeneously in silicone at the mass ratios of 1.0, 2.0, 3.0, 4.0, 5.0 and 6.0 wt %, and then coated on the surface of 450 nm-emitting GaN chips until the reflective cavities were filled up; (ii) YAG:Ce was blended in silicone at a constant mass ratio of 1.0 wt %, and [(TPTA)₂Ir(dPPOA)]PF₆ was blended together at different mass ratios of 0.0, 0.5, 1.0 and 1.5 wt %. The silicone containing YAG:Ce and [(TPTA)₂Ir(dPPOA)]PF₆ was also coated on the surface of 450 nm-emitting GaN chips until the reflective cavities were filled up. In the blending process, an analytical balance with the readability of 0.01 mg was used for weighing, 0.10000–0.12000 g viscous silicone was weighed in a little bottle every time, then the quantities of [(TPTA)₂Ir(dPPOA)]PF₆ and/or YAG:Ce were calculated and weighed. After [(TPTA)₂Ir(dPPOA)]PF₆ and/or YAG:Ce were added to the silicone, a drop of CH₂Cl₂ was also added, then the mixture was stirred by hand with a little stainless steel rod for about one minute until all the ingredients were well combined. The LEDs were dried and solidified at 150 °C for 1 h. The LEDs were all operated at 20 mA forward current and 5 V reverse voltage, with their performances measured by an integrating sphere spectroradiometer system (Everfine PMS-50, Everfine Photo-E-Info Co., Ltd., Hangzhou, China).

3. Results and Discussion

3.1. UV-Vis Absorption Spectra

The normalized UV-vis absorption spectrum of [(TPTA)₂Ir(dPPOA)]PF₆ in CH₂Cl₂ solution at 1.0×10^{-5} mol·L^{−1} together with the emission spectra of the blue GaN chip and YAG:Ce are shown in Figure 2. The strong absorption band between 230 nm and 380 nm can be ascribed to

the spin-allowed $^1\pi-\pi^*$ transition of the ligands; the maximum absorption wavelength ($\lambda_{\text{abs, max}}$) is 267 nm ($\epsilon_{267\text{nm}} = 5.4 \times 10^4 \text{ L}\cdot\text{mol}^{-1}\cdot\text{cm}^{-1}$). The weak absorption band from 380 nm extending to the visible region results from the overlapping absorption of the spin-allowed singlet metal-to-ligand charge-transfer ($^1\text{MLCT}$), the spin-forbidden triplet metal-to-ligand charge-transfer ($^3\text{MLCT}$) and $^3\pi-\pi^*$ in the ligands [25,34]. The admixture absorption of $^3\text{MLCT}$ and $^3\pi-\pi^*$ with higher-lying $^1\text{MLCT}$ is caused by the strong spin-orbit coupling induced by the heavy iridium atom [35,36]. As shown in Figure 2, there is a large overlap between the absorption spectrum of $[(\text{TPTA})_2\text{Ir}(\text{dPPOA})]\text{PF}_6$ and the emission spectrum of the blue GaN chip ($\lambda_{\text{em, max}} = 450 \text{ nm}$), which suggests that Förster resonance energy transfer (FRET) is able to take place between them easily and $[(\text{TPTA})_2\text{Ir}(\text{dPPOA})]\text{PF}_6$ can be well excited by the blue GaN chip [37]. The overlap between the absorption spectrum of $[(\text{TPTA})_2\text{Ir}(\text{dPPOA})]\text{PF}_6$ and the emission spectrum of YAG:Ce can almost be ignored, which suggests that the emission of YAG:Ce would be seldom affected by $[(\text{TPTA})_2\text{Ir}(\text{dPPOA})]\text{PF}_6$, and $[(\text{TPTA})_2\text{Ir}(\text{dPPOA})]\text{PF}_6$ is a practicable red luminescent additive for YAG:Ce-based WLEDs.

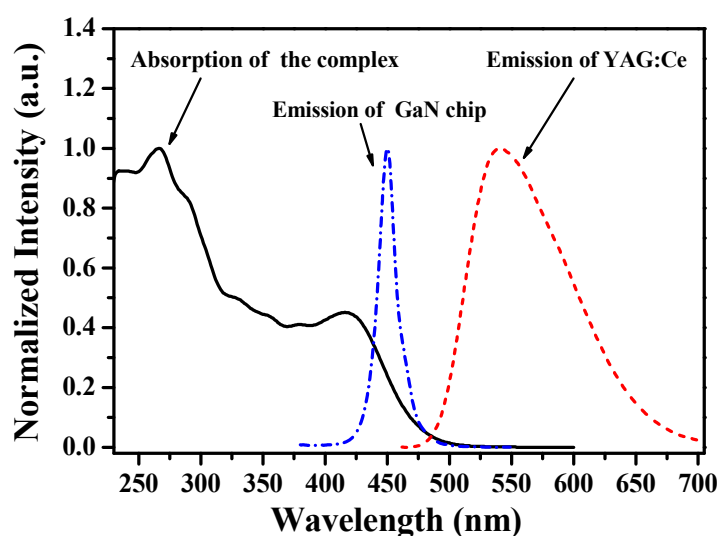


Figure 2. Normalized UV-vis absorption spectrum of $[(\text{TPTA})_2\text{Ir}(\text{dPPOA})]\text{PF}_6$ in CH_2Cl_2 solution at $1.0 \times 10^{-5} \text{ mol}\cdot\text{L}^{-1}$ and emission spectra of the blue GaN chip and YAG:Ce.

3.2. Photoluminescent Properties

The photoluminescent properties of $[(\text{TPTA})_2\text{Ir}(\text{dPPOA})]\text{PF}_6$ in solution and blended in silicone were investigated and the results are shown in Figure 3. Both excitation (Ex , $\lambda_{\text{em}} = 600 \text{ nm}$) and emission (Em , $\lambda_{\text{ex}} = 450 \text{ nm}$) spectra of $[(\text{TPTA})_2\text{Ir}(\text{dPPOA})]\text{PF}_6$ in silicone showed obvious red shift in comparison with those of $[(\text{TPTA})_2\text{Ir}(\text{dPPOA})]\text{PF}_6$ in CH_2Cl_2 solution ($\lambda_{\text{em}} = 581 \text{ nm}$, $\lambda_{\text{ex}} = 450 \text{ nm}$). The red shift should be caused mainly by the increase of the conjugated system of $[(\text{TPTA})_2\text{Ir}(\text{dPPOA})]\text{PF}_6$ in solid silicone, because the steric hindrance and distortion of the phenyls in ligands TPTA and dPPOA are restrained to a certain degree. At the same time, the conjugated system of $[(\text{TPTA})_2\text{Ir}(\text{dPPOA})]\text{PF}_6$ can also be increased by intermolecular $\pi-\pi$ stacking in silicone.

In general, sufficient overlap between the excitation spectra of phosphors and the emission spectra of the LED chips is necessary to realize energy transfer from the LED chips to phosphors efficiently. In this work, the excitation spectra of $[(\text{TPTA})_2\text{Ir}(\text{dPPOA})]\text{PF}_6$ in CH_2Cl_2 solution and blended in silicone lie 225–500 nm and 225–580 nm respectively, and both cover the emission spectra of the 450 nm-emitting blue GaN chip (as shown in Figure 2), which means that $[(\text{TPTA})_2\text{Ir}(\text{dPPOA})]\text{PF}_6$ can be efficiently excited by the blue GaN chip. In particular, there is a maximum wavelength (448 nm) near 450 nm in the excitation spectra of $[(\text{TPTA})_2\text{Ir}(\text{dPPOA})]\text{PF}_6$ blended in silicone, which suggests that the $[(\text{TPTA})_2\text{Ir}(\text{dPPOA})]\text{PF}_6$ can be efficiently excited by the blue light of the GaN chip. The emission spectra of $[(\text{TPTA})_2\text{Ir}(\text{dPPOA})]\text{PF}_6$ mainly lie from 520 nm to 750 nm with the maximum emission

wavelengths of 581 nm (in solution) and 600 nm (in silicone) respectively; obviously, considerable red light component was contained in its emission spectra and $[(\text{TPTA})_2\text{Ir}(\text{dPPOA})]\text{PF}_6$ can be used as a phosphor for fabricating warm WLEDs.

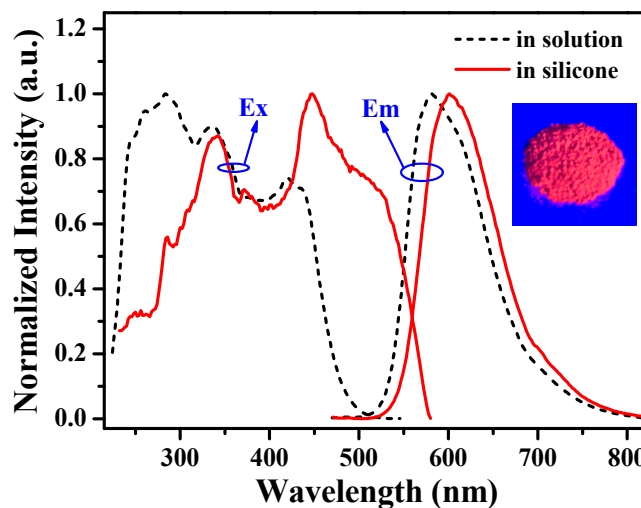


Figure 3. Normalized excitation (Ex, $\lambda_{\text{em}} = 581, 600$ nm) and emission (Em, $\lambda_{\text{ex}} = 450$ nm) spectra of $[(\text{TPTA})_2\text{Ir}(\text{dPPOA})]\text{PF}_6$ in CH_2Cl_2 solution at $1.0 \times 10^{-5} \text{ mol} \cdot \text{L}^{-1}$ and blended in silicone at 6.0 wt % (coated on quartz plate). Inset: A photograph of $[(\text{TPTA})_2\text{Ir}(\text{dPPOA})]\text{PF}_6$ powders excited by blue light ($\lambda_{\text{ex}} = 450$ nm).

3.3. Thermal Stability and Thermal Quenching Properties

The thermal property of $[(\text{TPTA})_2\text{Ir}(\text{dPPOA})]\text{PF}_6$ was characterized by thermogravimetry (TG) in nitrogen atmosphere at a heating speed of $10.0 \text{ }^\circ\text{C} \cdot \text{min}^{-1}$, and the resultant TG curve is shown in Figure 4. With temperature increasing, the TG curve begins to dip suddenly after about $375 \text{ }^\circ\text{C}$, which means that the thermal decomposition happened and $375 \text{ }^\circ\text{C}$ can be regarded as its thermal decomposition temperature (T_d). Such a high decomposition temperature suggests that $[(\text{TPTA})_2\text{Ir}(\text{dPPOA})]\text{PF}_6$ has a high thermal stability and is enough to meet the requirement of its application in LEDs, since LED devices are fabricated and usually work at a temperature below $150 \text{ }^\circ\text{C}$ [14].

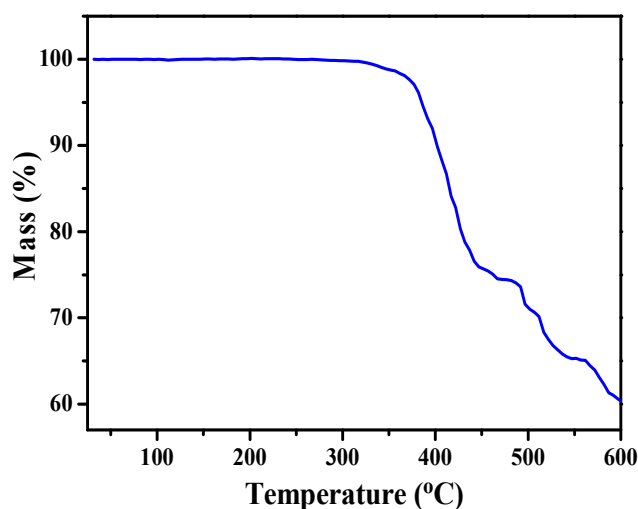


Figure 4. Thermogravimetric (TG) curve of $[(\text{TPTA})_2\text{Ir}(\text{dPPOA})]\text{PF}_6$.

The thermal-quenching property of $[(\text{TPTA})_2\text{Ir}(\text{dPPOA})]\text{PF}_6$ was also investigated and the results are shown in Figures 5 and 6. Figure 5 depicts the temperature-dependent photoluminescent spectra ($\lambda_{\text{ex}} = 450 \text{ nm}$) of $[(\text{TPTA})_2\text{Ir}(\text{dPPOA})]\text{PF}_6$ powders. From 25°C to 200°C , the light-emitting color of $[(\text{TPTA})_2\text{Ir}(\text{dPPOA})]\text{PF}_6$ exhibited high thermal stability because the profile, wavelength band and the maximum wavelengths (around 601 nm) of its emission spectra at different temperatures were almost unchanged, with the exception of the intensity. The relative emission intensity of $[(\text{TPTA})_2\text{Ir}(\text{dPPOA})]\text{PF}_6$ as a function of temperature is shown in Figure 6. Like most phosphors used in LEDs, the emission intensity of $[(\text{TPTA})_2\text{Ir}(\text{dPPOA})]\text{PF}_6$ also decreases with increasing temperature (i.e., thermal quenching) [4,38–40]. The relative emission intensities at different temperatures are descending: 97.2% (at 50°C), 93.7% (at 75°C), 88.8% (at 100°C), 82.3% (at 125°C), 76.5% (at 150°C), 68.9% (at 175°C), 61.9% (at 200°C). The thermal quenching of luminescent organic metal complexes is usually caused by the aggravating jiggle and wiggle of atoms, and the rotating and stretching vibration of covalent bonds as the temperature increases. The activation energy (E_a) of the thermal quenching can be described by the Arrhenius equation [38–40]:

$$I = \frac{I_0}{1 + A \exp(-\frac{E_a}{k_B T})}$$

where I represents the emission intensity at any testing temperature ($25\text{--}200^\circ\text{C}$), I_0 represents the emission intensity at room temperature (25°C), A is a constant, k_B is a Boltzmann constant, and T is any testing temperature. From the Arrhenius equation, the relationship of $\ln(I_0/I - 1)$ with $1/T$ can be obtained; the experimental data are well-fitted and shown in Figure 6 (inset); then, the value of E_a for $[(\text{TPTA})_2\text{Ir}(\text{dPPOA})]\text{PF}_6$ was calculated to be 0.2647 eV from the slope value $-(E_a/k_B)$. For phosphors used in LEDs, a high E_a value means low thermal quenching. The emission intensity decay rate and E_a value show that $[(\text{TPTA})_2\text{Ir}(\text{dPPOA})]\text{PF}_6$ is an applicable phosphor for LEDs and its thermal quenching is lower than that of many orange or red phosphors reported in recent years [40–42].

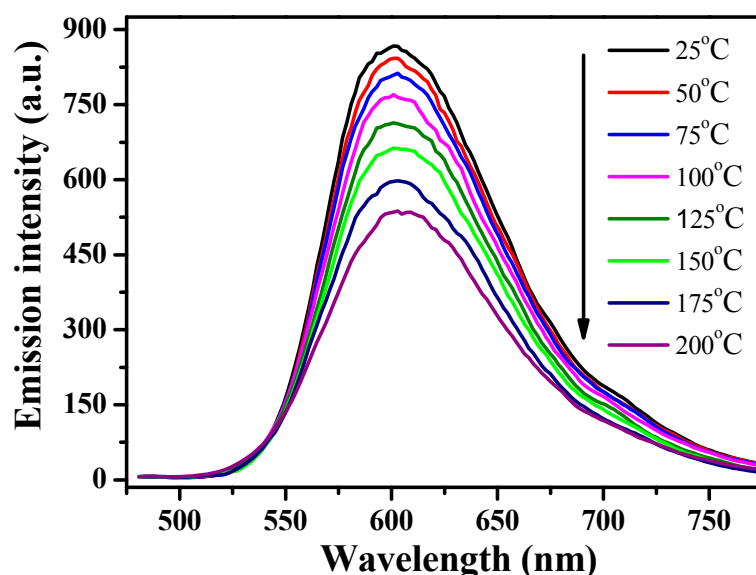


Figure 5. Temperature-dependent photoluminescent emission spectra of $[(\text{TPTA})_2\text{Ir}(\text{dPPOA})]\text{PF}_6$ powders measured with increasing temperature from 25°C to 200°C , $\lambda_{\text{ex}} = 450 \text{ nm}$.

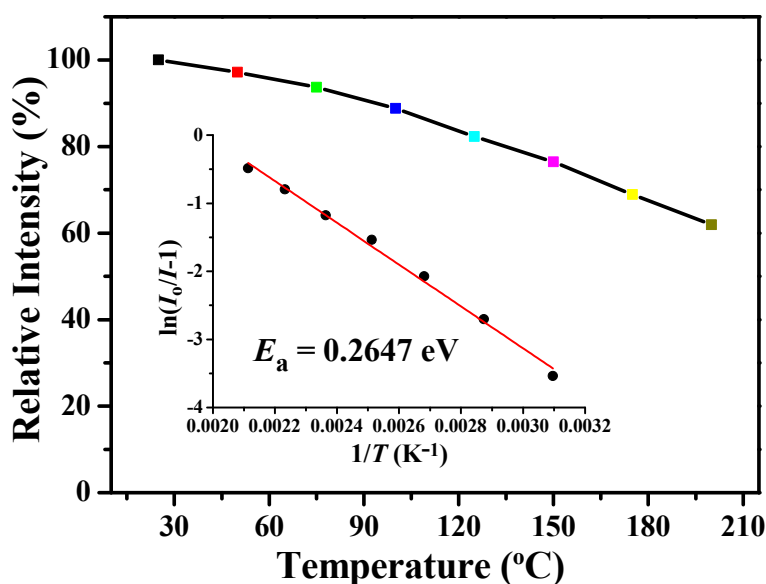


Figure 6. Relative emission intensity of $[(\text{TPTA})_2\text{Ir}(\text{dPPOA})]\text{PF}_6$ as a function of temperature. The inset represents the $\ln(I_0/I - 1)$ versus $1/T$ and the calculated activation energy (E_a) for $[(\text{TPTA})_2\text{Ir}(\text{dPPOA})]\text{PF}_6$.

3.4. Fabrication and Performance of LEDs

At first, in order to understand the luminescent property of $[(\text{TPTA})_2\text{Ir}(\text{dPPOA})]\text{PF}_6$ itself in LEDs, a series of LEDs fabricated using blue GaN (450 nm) as chips and only $[(\text{TPTA})_2\text{Ir}(\text{dPPOA})]\text{PF}_6$ as a phosphor at different blending concentrations were investigated. The emission spectra of such LEDs at 20 mA forward current are shown in Figure 7 and the performances are listed in Table 1. Except for the emission spectrum of the LED using $[(\text{TPTA})_2\text{Ir}(\text{dPPOA})]\text{PF}_6$ at 6.0 wt %, two emission peaks were contained in the emission spectra of the other LEDs. Obviously, the blue emission peaks on the left with the maximum wavelengths around 450 nm were the emission of the blue GaN chips, which were not completely absorbed by $[(\text{TPTA})_2\text{Ir}(\text{dPPOA})]\text{PF}_6$ at low blending concentrations. The broad emission peaks (550–770 nm) on the right with the maximum wavelengths around 615 nm can be ascribed to the emission of $[(\text{TPTA})_2\text{Ir}(\text{dPPOA})]\text{PF}_6$ because they were primarily consistent with the PL spectra of $[(\text{TPTA})_2\text{Ir}(\text{dPPOA})]\text{PF}_6$. The blending concentrations of $[(\text{TPTA})_2\text{Ir}(\text{dPPOA})]\text{PF}_6$ increased from 1.0 wt % to 6.0 wt %, while the emission peaks of blue GaN chips gradually declined and eventually disappeared at 6.0 wt %. On the other hand, the emission peaks of $[(\text{TPTA})_2\text{Ir}(\text{dPPOA})]\text{PF}_6$ gradually increased; at 6.0 wt %, only orange light of $[(\text{TPTA})_2\text{Ir}(\text{dPPOA})]\text{PF}_6$ emitted from the LED; the CIE (Commission Internationale de L'Eclairage) chromaticity coordinates of this LED was (0.62, 0.38), the CRI was 48.0 and the CCT was 1265 K. These results show that $[(\text{TPTA})_2\text{Ir}(\text{dPPOA})]\text{PF}_6$ can be efficiently excited by blue GaN (450 nm) chips, and it is a potential red-light-source phosphor for changing the cold white light of aforementioned YAG:Ce-based WLEDs into warm white light.

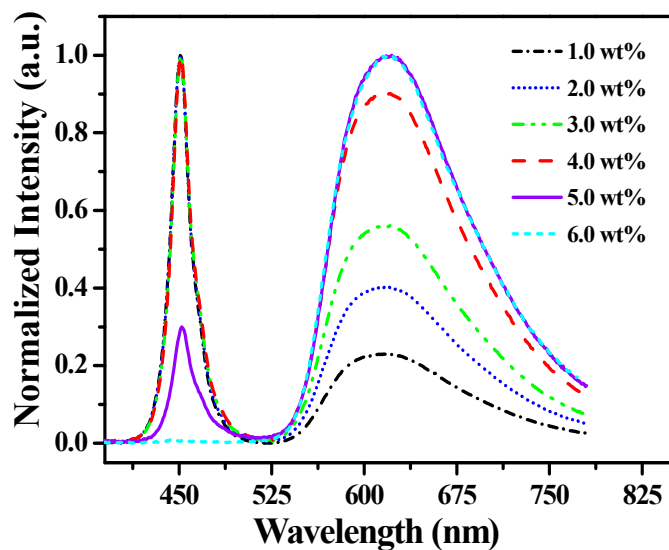


Figure 7. Emission spectra of light-emitting diodes (LEDs) using blue GaN as chips and only [(TPTA)₂Ir(dPPOA)]PF₆ as a phosphor at different blending concentrations at 20 mA forward current.

Table 1. Performances of blue GaN-based LEDs only using [(TPTA)₂Ir(dPPOA)]PF₆ as a phosphor at different blending concentrations (at 20 mA forward current).

No. of LEDs	Blending Concentration (wt %)	Luminous Efficiency (lm·W ⁻¹)	CRI	CCT (K)	λ _{em, max} (nm)	CIE (x, y)
a	1.0	18.9	31.6	100,000	451, 609	(0.31, 0.17)
b	2.0	15.8	40.7	2159	451, 610	(0.37, 0.21)
c	3.0	12.1	46.6	1957	451, 614	(0.41, 0.25)
d	4.0	10.1	50.2	1737	451, 617	(0.45, 0.28)
e	5.0	7.3	51.6	1507	451, 619	(0.55, 0.35)
f	6.0	5.4	48.0	1265	619	(0.62, 0.38)

In order to demonstrate the application of [(TPTA)₂Ir(dPPOA)]PF₆ for WLEDs, a series of blue GaN-based WLEDs using YAG:Ce (1.0 wt %) and [(TPTA)₂Ir(dPPOA)]PF₆ (*x* wt %, *x* = 0.0, 0.5, 1.0, 1.5) as phosphors blended in silicone were fabricated and measured. The emission spectra of these WLEDs are shown in Figure 8 and their performances are listed in Table 2. As mentioned previously, the emission peaks of blue GaN chips were also on the left, and their maximum wavelengths were also around 450 nm. On the right, the broad emission peaks from 500 nm to 725 nm were the mixture of emissions from YAG:Ce and [(TPTA)₂Ir(dPPOA)]PF₆ at different concentrations respectively. Before [(TPTA)₂Ir(dPPOA)]PF₆ was blended in, the WLED (No. g) only using YAG:Ce as its phosphor exhibited high CCT (6877 K) and low CRI (72.2). After [(TPTA)₂Ir(dPPOA)]PF₆ was blended in, the emission peaks on the right showed visible red shift and became broader. When the blending concentrations increased from 0.0 wt % to 1.5 wt %, the maximum wavelengths changed from 554 nm (No. g) to 571 nm (No. h), and then to 582 nm (No. i) and 586 nm (No. j); at the same time, the intensity of the right emission peaks also increased with the increase of the blending concentrations of [(TPTA)₂Ir(dPPOA)]PF₆. The correlated color temperatures (CCTs) of WLEDs using [(TPTA)₂Ir(dPPOA)]PF₆ at 0.5 wt % (No. h), 1.0 wt % (No. i) and 1.5 wt % (No. j) were 4896 K, 3473 K and 2864 K respectively; obviously, the CCTs declined in order with the increase of blending concentrations. The CRIs of WLEDs No. h, i and j were 78.4, 80.2 and 75.7 respectively; all of them were higher than the CRI (72.2) of the WLED No. g without [(TPTA)₂Ir(dPPOA)]PF₆.

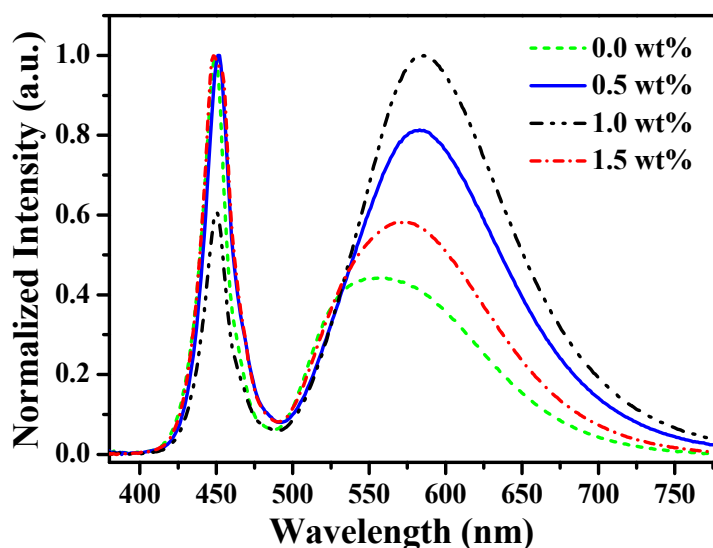


Figure 8. Emission spectra of blue GaN-based white light-emitting diodes (WLEDs) using YAG:Ce (1.0 wt %) and [(TPTA)₂Ir(dPPOA)]PF₆ (*x* wt %, *x* = 0.0, 0.5, 1.0, 1.5) as phosphors blended insilicone at different concentrations.

Table 2. Performances of WLEDs fabricated by using YAG:Ce and [(TPTA)₂Ir(dPPOA)]PF₆ as phosphors (at 20 mA forward current).

No. of LEDs	Blending Concentration (wt %)		Luminous Efficiency (lm·W ^{−1})	CRI	CCT (K)	λ _{em, max} (nm)	CIE (<i>x</i> , <i>y</i>)
	YAG:Ce	Complex					
g	1.0	0.0	128.5	72.2	6877	449, 556	(0.32, 0.33)
h	1.0	0.5	85.2	78.4	4896	448, 573	(0.35, 0.33)
i	1.0	1.0	46.1	80.2	3473	451, 583	(0.39, 0.36)
j	1.0	1.5	45.3	75.7	2864	450, 586	(0.44, 0.40)

The luminous efficiencies of WLEDs No. h, i and j were 85.2 lm·W^{−1}, 46.1 lm·W^{−1} and 45.3 lm·W^{−1} respectively. In contrast with WLED No. g (128.5 lm·W^{−1}), the luminous efficiencies decreased due to energy loss in light conversion. Besides some loss of luminous efficiencies when blue light was directly absorbed by [(TPTA)₂Ir(dPPOA)]PF₆ and transformed into orange light, some of the yellow light emitted from YAG:Ce was also absorbed by [(TPTA)₂Ir(dPPOA)]PF₆. Consequently, there was also a loss of luminous. Due to some degree of overlap between the excitation spectra of the iridium complex in silicone and the emission spectra of YAG:Ce (Figures 2 and 3), such secondary light energy conversion aggravated the loss of total luminous efficiencies of the LEDs. By comparison with [Ir(CBT)₂(dPPOA)]PF₆ which was also used as a red-light-source phosphor in warm WLEDs in our previous work [15], the WLEDs using [Ir(CBT)₂(dPPOA)]PF₆ exhibited lower loss of luminous efficiencies. Thus, the aforementioned secondary light energy conversion between YAG:Ce and the iridium(III) complex can be ignored, mainly because ligand TPTA make wider excitation spectra for [(TPTA)₂Ir(dPPOA)]PF₆ than that of CBT for [Ir(CBT)₂(dPPOA)]PF₆. The excitation spectra of [Ir(CBT)₂(dPPOA)]PF₆ have much lower overlap with the emission spectra of YAG:Ce. Even so, the remaining efficiencies were still encouraging. Moreover, the CRIs of No. h, i and j have been improved, the CCTs of No. h, i and j have been lowered significantly and warmer white lights are obtained. The light emitted from WLED No. h became neutral white light, while the light emitted from WLEDs No. i and j were both warm white light. The CIE chromaticity coordinates of WLEDs No. g, h, i and j were (0.32, 0.33), (0.35, 0.33), (0.39, 0.36) and (0.44, 0.40), respectively. Their CIE chromaticity coordinates and working state photographs are all shown in Figure 9 to visually exhibit the aforementioned changes. In order to further exhibit the changes, the CIE chromaticity coordinates

and working state photograph of the orange LED (No. f, only using $[(\text{TPTA})_2\text{Ir}(\text{dPPOA})]\text{PF}_6$ as a phosphor at 6.0 wt %) is also shown in Figure 9, because WLEDs No. h, i and j can be regarded as intermediate devices between WLEDs No. h and orange LED No. f.

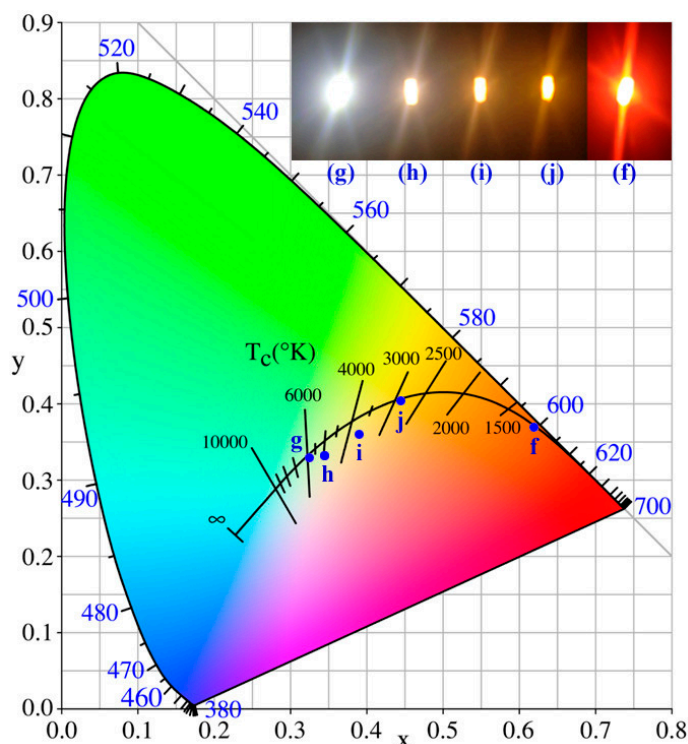


Figure 9. CIE chromaticity coordinates of blue GaN-based LEDs using YAG:Ce and $[(\text{TPTA})_2\text{Ir}(\text{dPPOA})]\text{PF}_6$ as phosphors at different blending concentrations. (f) only $[(\text{TPTA})_2\text{Ir}(\text{dPPOA})]\text{PF}_6$ at 6.0 wt %; (g) only YAG:Ce at 1.0 wt %; (h) 1.0 wt % YAG:Ce and 0.5 wt % $[(\text{TPTA})_2\text{Ir}(\text{dPPOA})]\text{PF}_6$; (i) 1.0 wt % YAG:Ce and 1.0 wt % $[(\text{TPTA})_2\text{Ir}(\text{dPPOA})]\text{PF}_6$; (j) 1.0 wt % YAG:Ce and 1.5 wt % $[(\text{TPTA})_2\text{Ir}(\text{dPPOA})]\text{PF}_6$. Inset: The photographs of the LEDs No. g, h, i, j and f in working state.

4. Conclusions

A novel orange cationic iridium(III) complex $[(\text{TPTA})_2\text{Ir}(\text{dPPOA})]\text{PF}_6$ was synthesized. The $[(\text{TPTA})_2\text{Ir}(\text{dPPOA})]\text{PF}_6$ complex has a high thermal stability with a decomposition temperature of 375 °C, and its relative emission intensity at 100 °C is 88.8% of that at 25 °C. The $[(\text{TPTA})_2\text{Ir}(\text{dPPOA})]\text{PF}_6$ complex can be efficiently excited by blue GaN (450 nm) chips. GaN-based cold white LEDs using only YAG:Ce as a phosphor can become neutral WLEDs and warm WLEDs when $[(\text{TPTA})_2\text{Ir}(\text{dPPOA})]\text{PF}_6$ is added at proper concentrations. The $[(\text{TPTA})_2\text{Ir}(\text{dPPOA})]\text{PF}_6$ complex can effectively improve the red light component for WLEDs, and is a promising phosphor candidate for warm WLEDs.

Supplementary Materials: The following are available online at www.mdpi.com/1996-1944/10/6/657/s1, Figure S1: ^1H NMR spectrum of $[(\text{TPTA})_2\text{Ir}(\text{POA})]\text{PF}_6$, Figure S2: MS spectrum of $[(\text{TPTA})_2\text{Ir}(\text{POA})]\text{PF}_6$.

Acknowledgments: This work was supported by National Nature Science Foundation of China (No. 21262046 and 21261027).

Author Contributions: Huaijun Tang, Guoyun Meng, Zeyu Chen and Kaijin Wang performed the experiments; Huaijun Tang, Guoyun Meng and Zhengliang Wang analyzed the data; and Huaijun Tang wrote the initial draft of the manuscript. Huaijun Tang and Zhengliang Wang designed and supervised the project, reviewed and contributed to the final revised manuscript. All authors contributed to the analysis and conclusion, and read the final paper.

Conflicts of Interest: The authors declare no conflict of interest.

References

1. Pimputkar, S.; Speck, J.S.; DenBaars, S.P.; Nakamura, S. Prospects for LED lighting. *Nat. Photonics* **2009**, *3*, 180–182. [[CrossRef](#)]
2. Tsao, J.Y.; Crawford, M.H.; Coltrin, M.E.; Fischer, A.J.; Koleske, D.D.; Subramania, G.S.; Wang, G.T.; Wierer, J.J.; Karliceck, R.F., Jr. Toward smart and ultra-efficient solid-state lighting. *Adv. Opt. Mater.* **2014**, *2*, 809–836. [[CrossRef](#)]
3. Feezell, D.F.; Speck, J.S.; DenBaars, S.P.; Nakamura, S. Semipolar (20-2-1) InGaN/GaN light-emitting diodes for high-efficiency solid-state lighting. *J. Disp. Technol.* **2013**, *9*, 190–198. [[CrossRef](#)]
4. Chen, L.; Lin, C.C.; Yeh, C.W.; Liu, R.S. Light converting inorganic phosphors for white light-emitting diodes. *Materials* **2010**, *3*, 2172–2195. [[CrossRef](#)]
5. Jang, H.S.; Won, Y.-H.; Jeon, D.Y. Improvement of electroluminescent property of blue LED coated with highly luminescent yellow-emitting phosphors. *Appl. Phys. B* **2009**, *95*, 715–720. [[CrossRef](#)]
6. Zhu, H.; Lin, C.C.; Luo, W.; Shu, S.; Liu, Z.; Liu, Y.; Kong, J.; Ma, E.; Cao, Y.; Liu, R.-S.; et al. Highly efficient non-rare-earth red emitting phosphor for warm white light-emitting diodes. *Nat. Commun.* **2014**, *5*, 4312. [[CrossRef](#)] [[PubMed](#)]
7. Kwak, H.H.; Kim, S.J.; Park, Y.S.; Yoon, H.H.; Park, S.J.; Choi, H.W. Photoluminescence Characteristic of Ce³⁺-Eu³⁺ Co-doped Y₃Al₅O₁₂ Phosphor Prepared by Combustion Method. *Mol. Cryst. Liq. Cryst.* **2009**, *513*, 106–113. [[CrossRef](#)]
8. Jang, H.S.; Im, W.B.; Lee, D.C.; Jeon, D.Y.; Kim, S.S. Enhancement of red spectral emission intensity of Y₃Al₅O₁₂:Ce³⁺ phosphor via Pr Co-doping and Tb substitution for the application to white LEDs. *J. Lumin.* **2007**, *126*, 371–377. [[CrossRef](#)]
9. Wang, X.; Zhou, G.; Zhang, H.L.; Li, H.; Zhang, Z.; Sun, Z. Luminescent properties of yellowish orange Y₃Al_{5-x}Si_xO_{12-x}N_x: Ce phosphors and their applications in warm white light-emitting diodes. *J. Alloys Compd.* **2012**, *519*, 149–155. [[CrossRef](#)]
10. Lin, C.C.; Zheng, Y.S.; Chen, H.Y.; Ruan, C.H.; Xiao, G.W.; Liu, R.S. Improving optical properties of white LED fabricated by a blue LED chip with yellow/red phosphors. *J. Electrochem. Soc.* **2010**, *157*, 900–903. [[CrossRef](#)]
11. Kim, S.; Kim, T.; Kang, M.; Kwak, S.K.; Yoo, T.W.; Park, L.S.; Yang, I.; Hwang, S.; Lee, J.E.; Kim, S.K.; et al. Highly luminescent InP/GaP/ZnS nanocrystals and their application to white light-emitting diodes. *J. Am. Chem. Soc.* **2012**, *134*, 3804–3809. [[CrossRef](#)] [[PubMed](#)]
12. Zhou, Q.; Tan, H.; Zhou, Y.; Zhang, Q.; Wang, Z.; Yan, J.; Wu, M. Optical performance of Mn⁴⁺ in a new hexa-coordinated fluorozirconate complex of Cs₂ZrF₆. *J. Mater. Chem. C* **2016**, *4*, 7443–7448. [[CrossRef](#)]
13. Tan, H.; Rong, M.; Zhou, Y.; Yang, Z.; Wang, Z.; Zhang, Q.; Wang, Q.; Zhou, Q. Luminescence behaviour of Mn⁴⁺ ions in seven coordination environments of K₃ZrF₇. *Dalton Trans.* **2016**, *45*, 9654–9660. [[CrossRef](#)] [[PubMed](#)]
14. Wang, H.; He, P.; Liu, S.; Shi, J.; Gong, M. A europium(III) organic ternary complex applied in fabrication of near UV-based white light-emitting diodes. *Appl. Phys. B* **2009**, *97*, 481–487. [[CrossRef](#)]
15. Meng, G.; Chen, Z.; Tang, H.; Liu, Y.; Wei, L.; Wang, Z. A novel cationic iridium(III) complex as red phosphor applied in warm white light-emitting diodes. *New J. Chem.* **2015**, *39*, 9535–9542. [[CrossRef](#)]
16. Luo, Y.; Yan, Q.; Zhang, Z.; Yu, X.; Wu, W.; Su, W.; Zhang, Q. White LED based on poly(N-vinylcarbazole) and lanthanide complexes ternary co-doping system. *J. Photochem. Photobiol. A* **2009**, *206*, 102–108. [[CrossRef](#)]
17. Xiang, H.-F.; Yu, S.-C.; Che, C.-M.; Lai, P.T. Efficient white and red light emission from GaN/tris-(8-hydroxyquinolato) aluminum/platinum(II) meso-tetrakis(pentafluorophenyl) porphyrin hybrid light-emitting diodes. *Appl. Phys. Lett.* **2003**, *83*, 1518–1520. [[CrossRef](#)]
18. Niklaus, L.; Dakhil, H.; Kostrzewa, M.; Coto, P.B.; Sonnewald, U.; Wierschem, A.; Costa, R.D. Easy and versatile coating approach for long-living white hybrid light-emitting diodes. *Mater. Horiz.* **2016**, *3*, 340–347. [[CrossRef](#)]
19. Zhang, C.; Heeger, A.J. Gallium nitride/conjugated polymer hybrid light emitting diodes: Performance and lifetime. *J. Appl. Phys.* **1998**, *84*, 1579–1582. [[CrossRef](#)]

20. Martino, D.D.; Beverina, L.; Sassi, M.; Brovelli, S.; Tubino, R.; Meinardi, F. Straightforward fabrication of stable white LEDs by embedding of inorganic UV-LEDs into bulk polymerized polymethyl-methacrylate doped with organic dyes. *Sci. Rep.* **2014**, *4*, 4400. [[CrossRef](#)] [[PubMed](#)]
21. Jin, J.-Y.; Kim, H.-G.; Hong, C.-H.; Suh, E.-K.; Lee, Y.-S. White light emission from a blue LED, combined with a sodium salt of fluorescein dye. *Synth. Met.* **2007**, *157*, 138–141. [[CrossRef](#)]
22. Costa, R.D.; Orti, E.; Bolink, H.J.; Monti, F.; Accorsi, G.; Armaroli, N. Luminescent ionic transition-metal complexes for light-emitting electrochemical cells. *Angew. Chem. Int. Ed.* **2012**, *51*, 8178–8211. [[CrossRef](#)] [[PubMed](#)]
23. Hu, T.; He, L.; Duan, L.; Qiu, Y. Solid-state light-emitting electrochemical cells based on ionic iridium(III) complexes. *J. Mater. Chem.* **2012**, *22*, 4206–4215. [[CrossRef](#)]
24. Ma, D.; Tsuboi, T.; Qiu, Y.; Duan, L. Recent progress in ionic iridium(III) complexes for organic electronic devices. *Adv. Mater.* **2017**, *29*, 1603253. [[CrossRef](#)] [[PubMed](#)]
25. Tang, H.; Li, Y.; Chen, Q.; Chen, B.; Qiao, Q.; Yang, W.; Wu, H.; Cao, Y. Efficient yellow-green light-emitting cationic iridium complexes based on 1,10-phenanthroline derivatives containing oxadiazol-triphenylamine unit. *Dyes Pigments* **2014**, *100*, 79–86. [[CrossRef](#)]
26. Tang, H.; Li, Y.; Zhao, B.; Yang, W.; Wu, H.; Cao, Y. Two novel orange cationic iridium(III) complexes with multifunctional ancillary ligands used for polymer light-emitting diodes. *Org. Electron.* **2012**, *13*, 3211–3219. [[CrossRef](#)]
27. Lo, K.K.-W.; Li, S.P.-Y.; Zhang, K.Y. Development of luminescent iridium(III) polypyridine complexes as chemical and biological probes. *New J. Chem.* **2011**, *35*, 265–287. [[CrossRef](#)]
28. Yang, Y.; Zhao, Q.; Feng, W.; Li, F. Luminescent chemodosimeters for bioimaging. *Chem. Rev.* **2013**, *113*, 192–270. [[CrossRef](#)] [[PubMed](#)]
29. Sun, C.-Y.; Wang, X.-L.; Zhang, X.; Qin, C.; Li, P.; Su, Z.-M.; Zhu, D.-X.; Shan, G.-G.; Shao, K.-Z.; Wu, H.; et al. Efficient and tunable white-light emission of metal-organic frameworks by iridium-complex encapsulation. *Nat. Commun.* **2013**, *4*, 2717. [[CrossRef](#)] [[PubMed](#)]
30. Yang, H.; Meng, G.; Zhou, Y.; Tang, H.; Zhao, J.; Wang, Z. The photoluminescent properties of new cationic iridium (III) complexes using different anions and their applications in white light-emitting diodes. *Materials* **2015**, *8*, 6105–6116. [[CrossRef](#)]
31. Dong, H.; Zhu, H.; Meng, Q.; Gong, X.; Hu, W. Organic photoresponse materials and devices. *Chem. Soc. Rev.* **2012**, *41*, 1754–1808. [[CrossRef](#)] [[PubMed](#)]
32. Lin, Y.; Li, Y.; Zhan, X. Small molecule semiconductors for high-efficiency organic photovoltaics. *Chem. Soc. Rev.* **2012**, *41*, 4245–4272. [[CrossRef](#)] [[PubMed](#)]
33. Chen, X.; Liu, R.; Xu, Y.; Zou, G. Tunable protic ionic liquids as solvent-catalysts for improved synthesis of multiply substituted 1,2,4-triazoles from oxadiazoles and organoamines. *Tetrahedron* **2012**, *68*, 4813–4819. [[CrossRef](#)]
34. Lowry, M.S.; Hudson, W.R.; Pascal, R.A., Jr.; Bernhard, S. Accelerated luminophore discovery through combinatorial synthesis. *J. Am. Chem. Soc.* **2004**, *126*, 14129–14135. [[CrossRef](#)] [[PubMed](#)]
35. Lamansky, S.; Djurovich, P.; Murphy, D.; Abdel-Razzaq, F.; Lee, H.-E.; Adachi, C.; Burrows, P.E.; Forrest, S.R.; Thompson, M.E. Highly phosphorescent bis-cyclometalated iridium complexes: Synthesis, photophysical characterization, and use in organic light emitting diodes. *J. Am. Chem. Soc.* **2001**, *123*, 4304–4312. [[CrossRef](#)] [[PubMed](#)]
36. Wong, W.-Y.; Zhou, G.-J.; Yu, X.-M.; Kwok, H.-S.; Lin, Z.-Y. Efficient organic light-emitting diodes based on sublimable charged iridium phosphorescent emitters. *Adv. Funct. Mater.* **2007**, *17*, 315–323. [[CrossRef](#)]
37. Sahoo, H. Förster resonance energy transfer—A spectroscopic nanoruler: Principle and applications. *J. Photochem. Photobiol. C* **2011**, *12*, 20–30. [[CrossRef](#)]
38. Lü, W.; Lv, W.; Zhao, Q.; Jiao, M.; Shao, B.; You, H. A novel efficient Mn⁴⁺ activated Ca₁₄Al₁₀Zn₆O₃₅ phosphor: Application in red-emitting and white LEDs. *Inorg. Chem.* **2014**, *53*, 11985–11990. [[CrossRef](#)] [[PubMed](#)]
39. Lee, S.-P.; Chan, T.-S.; Chen, T.-M. Novel reddish-orange-emitting BaLa₂Si₂S₈:Eu²⁺ thiosilicate phosphor for LED lighting. *ACS Appl. Mater. Interfaces* **2015**, *7*, 40–44. [[CrossRef](#)] [[PubMed](#)]
40. Ruan, J.; Xie, R.-J.; Hirosaki, N.; Takeda, T. Nitrogen gas pressure synthesis and photoluminescent properties of orange-red SrAlSi₄N₇:Eu²⁺ phosphors for white light-emitting diodes. *J. Am. Ceram. Soc.* **2011**, *94*, 536–542. [[CrossRef](#)]

41. Li, H.; Zhao, R.; Jia, Y.; Sun, W.; Fu, J.; Jiang, L.; Zhang, S.; Pang, R.; Li, C. $\text{Sr}_{1.7}\text{Zn}_{0.3}\text{CeO}_4\text{:Eu}^{3+}$ novel red-emitting phosphors: Synthesis and photoluminescence properties. *ACS Appl. Mater. Interfaces* **2014**, *6*, 3163–3169. [[CrossRef](#)] [[PubMed](#)]
42. Setlur, A.A.; Lyons, R.J.; Murphy, J.E.; Kumar, N.P.; Kishore, M.S. Blue light-emitting diode phosphors based upon oxide, oxyhalide, and halide hosts. *ECS J. Solid State Sci. Technol.* **2013**, *2*, R3059–R3070. [[CrossRef](#)]



© 2017 by the authors. Licensee MDPI, Basel, Switzerland. This article is an open access article distributed under the terms and conditions of the Creative Commons Attribution (CC BY) license (<http://creativecommons.org/licenses/by/4.0/>).